Comparative study of pulse interactions in optical fiber transmission systems with different modulation formats

O. V. Sinkin, J. Zweck, and C. R. Menyuk

University of Maryland Baltimore County, TRC 201-B, 5200 Westland Blvd., Baltimore, MD 21227

osinki1@umbc.edu
http://www.photonics.engr.umbc.edu/

Abstract: We compare nonlinear channel interactions in classical soliton, periodically-stationary dispersion-managed soliton (DMS), and chirped-return-to-zero (CRZ) systems. We studied multichannel systems with a single pulse in each channel and a more general case with multiple bit streams in each channel. First, we find that in classical soliton systems, the distortions are reversible, while in the DMS and CRZ systems they are not. Second, we find that the classical soliton system shows no increase in the degradation as the number of channels increases, while both the DMS and CRZ systems do show an increase in the degradation.

© 2001 Optical Society of America

OCIS codes: (060.2330) Fiber optics communications; (190.4380) Nonlinear optics, four-wave mixing

References

1. M. Suzuki, I. Morita, N. Edagawa, S. Yamamoto, H. Taga, and S. Akiba, "Reduction of Gordon-Hauss timing jitter by periodic dispersion compensation in soliton transmission," Electron. Lett. **31**, 2027–2029 (1995).
2. N. J. Smith, F. M. Knox, N. J. Doran, K. J. Blow and I. Bennion "Enhanced power solitons in optical fibres with periodic dispersion management," Electron. Lett. **32**, 54–55 (1996).
3. F. Le Guen, S. Del Burgo, M. L. Moulinard, D. Grot, M. Henry, F. Favre, and T. Georges, "Narrow band 1.02 Tbit/s (51x20 Gbit/s) soliton DWDM transmission over 1000 km of standard fiber with 100 km amplifier spans" in *Optical Fiber Communication Conference*, OSA Technical Digest (Optical Society of America, Washington DC, 1999), PD4.
4. A. Hasegawa, S. Kumar, and Y. Kodama, "Reduction of collision-induces timing jitters in dispersion-managed soliton transmission systems," Opt. Lett. **21**, 39–41 (1996).
5. N. S. Bergano, C. R. Davidson, M. A. Mills, P. Corbett, S. G. Evangelides, B. Pedersen, R. Menges, J. L. Zyskind, J. W. Sulhoff, A. K. Srivastava, C. Wolf, and J. Judkins, "Long-haul WDM transmission using optimal channel modulation" in *Optical Fiber Communication Conference*, OSA Technical Digest (Optical Society of America, Washington DC, 1997), PD16.
6. R.-M. Mu, T. Yu, V. S. Grigoryan, and C. R. Menyuk, "Convergence of the CRZ and DMS formats in WDM systems using dispersion management" in *Optical Fiber Communication Conference*, OSA Technical digest (Optical Society of America, Washington DC, 2000), FC1, 32–34.
7. C. R. Menyuk, "Application of multiple-length scale methods to the study of optical fiber transmission," J. Eng. Math. **36**, 113–136 (1999).
8. G. P. Agrawal, *Nonlinear Fiber Optics* (Academic, San Diego, CA 1995).
9. V. S. Grigoryan, C. R. Menyuk, and R.-M. Mu, "Calculation of timing and amplitude jitter in dispersion-managed optical fiber communications using linearization," J. Lightwave Technol. **17**, 1347–1356 (1999).
10. M. J. Ablowitz, G. Biondini, S. Chakravarty, R. B. Jenkins, and J. R. Sauer, "Four-wave mixing in wavelength-division-multiplexed soliton systems: ideal fibers," J. Opt. Soc. Am. B **14**, 1788–1794 (1997).
11. M. J. Ablowitz, G. Biondini, S. Chakravarty, R. B. Jenkins, and J. R. Sauer, "Four-wave mixing in wavelength-division-multiplexed soliton systems: damping and amplification," Opt. Lett. **21**, 1646–1648 (1996).

#35042 - $15.00 US Received August 27, 2001; Revised September 18, 2001
(C) 2001 OSA

12. A. Hasegawa, *Solitons in Optical Communications* (Clarendon Press, Oxford, NY 1995).
13. F. Foghieri, R. W. Tkach, A. R. Chraplyvy, "Fiber nonlinearities and their impact on transmission systems" in *Optical Fiber Telecommunications IIIA*, I. P. Kaminow and T. L. Koch, eds. (Academic, San Diego, CA 1997).

1 Introduction

One of the basic issues in the design of high-data rate optical fiber communications systems is to choose the data transmission format. Historically, fiber optic links inherited the conventional non-return-to-zero (NRZ) format from electronic communications systems, and this format remains the predominant modulation scheme at this time. On the other hand, optical solitons seem very attractive because of their stable pulse shape. In a fiber with anomalous dispersion, the nonlinearity and dispersion can balance, yielding a stationary pulse shape. However the combination of optical amplifier noise and high dispersion leads to a large timing jitter. To overcome this limitation, dispersion management was proposed for use in soliton systems, and it has been shown to significantly reduce timing jitter [1]. Dispersion-managed solitons (DMS) are similar in important respects to classical solitons. For example, the balance between the nonlinearity and dispersion is the key condition for the existence of periodically-stationary dispersion-managed solitons, enabling them to be propagated over thousands of kilometers. However, unlike classical solitons, the pulse shape repeats periodically [2] and is not stationary. In more recent work on quasilinear dispersion-managed soliton systems, the pulse shapes do not even repeat periodically [3]. In the presence of fiber loss and periodic lumped amplification, it is also possible to manage the dispersion using dispersion-tapered fiber for which the dispersion decreases exponentially with distance so that it matches the fiber loss [4]. In this case, one can mathematically transform the equations that govern the system so that they are identical to the equations that govern classical solitons, and the behavior is like that of classical soliton systems. Consequently, in this work, it is appropriate to compare pulse interactions in periodically-stationary DMS systems to those in classical soliton systems.

At the same time, the non-return-to-zero format has evolved into the chirped-return-to-zero (CRZ) format, where both amplitude and phase modulation are used to improve the system performance [5]. Even though the DMS and CRZ formats have very different origins, they have important similarities. Indeed, quasilinear DMS systems and CRZ systems appear difficult to distinguish in practice [6]. In this paper, when we refer to DMS systems, we always mean periodically-stationary DMS systems.

In WDM systems, pulses in different channels travel at different speeds due to dispersion, causing multiple collisions to occur. Due to the fiber nonlinearity these interactions result in pulse distortion and signal degradation, which limit the system performance. In this work, we compare interchannel interactions in WDM classical soliton, DMS, and CRZ systems using computer simulations. We demonstrate that in DMS systems the pulse interactions are qualitatively the same as in CRZ systems and are completely different from those of classical solitons. We start with a simple model in which only one pulse is launched in each channel. In the framework of this model, the collision dynamics and the effect of adding channels to a system are studied. We will demonstrate that adding channels generally decreases performance for the DMS and CRZ systems in contrast to classical solitons, where pulse collisions are elastic except for an overall time shift. Finally, we illustrate this effect using an animation of the eye diagram evolution for the classical solitons and the DMS system.

#35042 - $15.00 US Received August 27, 2001; Revised September 18, 2001
(C) 2001 OSA

2 Approach and methodology

2.1 *Simulation model*

The propagation of light in an optical fiber can be described by the nonlinear Schrödinger equation, which may be written as

$$i\frac{\partial q}{\partial z} \; - \; \frac{1}{2}\beta''(z)\frac{\partial^2 q}{\partial t^2} \; + \; \frac{i}{6}\beta'''(z)\frac{\partial^3 q}{\partial t^3} \; + \; \gamma|q|^2 q \; = \; i\Gamma(z)q, \tag{1}$$

where $q = q(z,t)$ is the electric field envelope, β'' is the second order dispersion, β''' is the third order dispersion, and z is physical distance. The quantity $t = T - \beta' z$ indicates retarded time, where T is the physical time and β' is the inverse group velocity. The factor $\Gamma(z)$ indicates amplification and loss, and $\gamma = n_2\omega_0/A_{\rm eff}c$ is the nonlinearity coefficient, where $n_2 = 2.6 \times 10^{-16}$ cm^2/W is the Kerr coefficient, ω_0 is the central frequency, $A_{\rm eff} = 47$ μm is the fiber effective area, and c is the speed of light. We do not consider polarization effects or noise. For a recent discussion of the conditions that must hold for the nonlinear Schrödinger equation to accurately model optical fiber transmission systems see ref. [7].

We begin our investigation of different modulation formats in WDM systems by focusing on the collision of two pulses in different wavelength channels. The two pulses are launched at two different frequencies and with a time offset so that they collide in the middle of the transmission line. We may thus write the initial field envelope as

$$q(z=0,t) = u(t-t_1)\exp(i\omega_1 t) + u(t-t_2)\exp(i\omega_2 t), \tag{2}$$

where $u(t)$ is the envelope of one of the pulses. In the case of classical solitons, the pulse shape has the form of a hyperbolic secant: $u(t) = \eta{\rm sech}(\eta t)$, where η is the pulse amplitude and inverse duration, which is related to the full width half maximum (FWHM) duration of the pulse power $|u(t)|^2$ by the formula $T_{\rm FWHM} = 2\ln(\sqrt{2}+1)/\eta$. In the DMS system, we use the Gaussian pulse shape: $u(t) = A\exp[-(t/t_0)^2]$ where A is the pulse amplitude and t_0 is pulse duration, which is related to the FWHM of the power $|u(t)|^2$ by $T_{\rm FWHM} = \sqrt{2\ln 2}\,t_0$. In the CRZ system the pulse has a raised-cosine shape of the form $u(t) = \sqrt{0.5P_0[1+\cos(2\pi t/T_{\rm bit})]}\exp[i\pi C\cos(2\pi t/T_{\rm bit})]$ for $-T_{\rm bit}/2 < t < T_{\rm bit}/2$ and $u(t) = 0$ elsewhere. The quantity P_0 is the peak power, $T_{\rm bit}$ is the bit period, and C is the chirp parameter. The FWHM duration of the pulse power is $T_{\rm FWHM} = T_{\rm bit}/2$. We solve (1) using the split-step Fourier method [8].

As the pulses propagate through the fiber, we calculate the evolution of the frequency sidebands that are generated by four-wave mixing. We use two quantities to measure the degree of interaction between pulses: sideband energy and pulse distortion. The sideband energy is defined as

$$\varepsilon_{\rm sb}(z) = \frac{\int_{\Omega_{\rm sb}} |\widetilde{q}(z,\omega)|^2 d\omega}{\int_{\Omega_1} |\widetilde{q}(z,\omega)|^2 d\omega}, \tag{3}$$

where $\Omega_{\rm sb} = [\omega_{\rm sb} - \Delta\omega/2,\, \omega_{\rm sb} + \Delta\omega/2]$ is the frequency band occupied by one of the sidebands, $\Omega_1 = [\omega_1 - \Delta\omega/2,\, \omega_1 + \Delta\omega/2]$ is the frequency range of the channel located at ω_1, $\Delta\omega$ is the channel spacing, and $\widetilde{q}(z,\omega)$ is the Fourier transform of $q(z,t)$. The pulse distortion is defined as

$$\delta(z) = \frac{\int_{\Omega_1} \Big||\widetilde{q}(z,\omega)| - |\widetilde{q}_1(z,\omega)|\Big| d\omega}{\int_{\Omega_1} |\widetilde{q}_1(z,\omega)| d\omega}, \tag{4}$$

where the envelope $\widetilde{q}_1(z,\omega)$ is the Fourier transform of one of the pulses envelopes $u(t-t_1)\exp(i\omega_1 t)$, propagating without the other. Thus $\delta(z)$ includes only the effects of

#35042 - $15.00 US Received August 27, 2001; Revised September 18, 2001
(C) 2001 OSA

distortion due to the collision. Note that a pure time shift leads to a frequency-dependent phase shift, which is removed by our use of the absolute value separately for $\widetilde{q}(z,\omega)$ and $\widetilde{q}_1(z,\omega)$. The pulse distortion $\delta(z)$ measures distortions due to the entire nonlinear Kerr effect, which includes self- and cross-phase modulation, as well as four-wave mixing.

2.2 *System design*

The purpose of this study is to compare interchannel interactions using the classical soliton, DMS, and CRZ modulation formats. We do not consider noise effects here.

The DMS system is based on a 200 km dispersion map, which consists of two fiber spans, each of 100 km, with normal dispersion equal to −2.19 ps/nm-km and anomalous dispersion of 2.35 ps/nm-km at 1550 nm [9]. These values correspond to 2.8 and −3.0 ps^2/km respectively. The loss in both fibers is 0.21 dB/km, and the amplifier spacing is 50 km. We use Gaussian pulses with a peak power of 1.5 mW, and we use a FWHM duration of 20 ps, as is appropriate for a 10 Gbit/s bit rate. The signal is launched in the middle of a span of anomalous fiber to ensure periodicity of the pulse shape as it propagates along the fiber. We do not consider the dispersion slope in this system.

The CRZ system is based on a 180 km dispersion map consisting of 160 km of dispersion-shifted fiber with dispersion −2.44 ps/nm-km, followed by 20 km of standard fiber with dispersion 16.55 ps/nm-km [5]. The dispersion slope is 0.075 ps^2/nm-km, and the fiber loss is 0.21 dB/km for both fibers, while the amplifier spacing is 45 km. Symmetric dispersion pre- and post-compensation is performed using fiber spans of length 9.8 km, with dispersion 93.5 ps/nm-km, slope −0.2 ps^2/nm-km, and loss 0.5 dB/km. The initial pulses are phase-modulated raised-cosine pulses with 1 mW peak power, 35 ps FWHM duration, and the chirp parameter C is −0.6.

The classical soliton system is based on a lossless fiber with an anomalous dispersion of 0.078 ps/nm-km. The dispersion slope is zero. The initial pulse has a hyperbolic secant shape with a peak power of 0.35 mW and a pulse duration of 20 ps. We stress that the soliton system is equivalent to a system that features fiber attenuation and an exponentially decreasing dispersion profile [4].

3 Results and discussion

3.1 *Two pulse collisions*

In this subsection we compare two-pulse collisions in different optical communication systems using the simulation model described in Section 2.1.

We begin with a demonstration of a collision of two classical solitons. The animation in Fig. 1 illustrates the collision dynamics. On the left we see the relative motion of two pulses at different frequencies. The time axis shows the normalized retarded time $\tau = t/T_0$, where T_0 is a characteristic time scale equal to 11.34 ps. This characteristic time corresponds to the duration $1/\eta$ of the hyperbolic secant pulse with $T_{\text{FWHM}} =$ 20 ps. On the right, we show the spectrum. The frequency axis shows the normalized frequency $\omega = 2\pi f T_0$, where f is the frequency. The slider at the bottom indicates the distance. At the beginning, we see two distinct frequencies in the spectrum. As the pulses approach each other in time, the sideband frequencies start growing. They reach a maximum at the point of maximum overlap around 5000 km, and they finally decay to zero when the pulses move apart.

This reabsorption of sideband energy is one of the remarkable properties of classical solitons and is due to their high degree of symmetry [10]. Note that if we used fibers with

#35042 - $15.00 US Received August 27, 2001; Revised September 18, 2001
(C) 2001 OSA

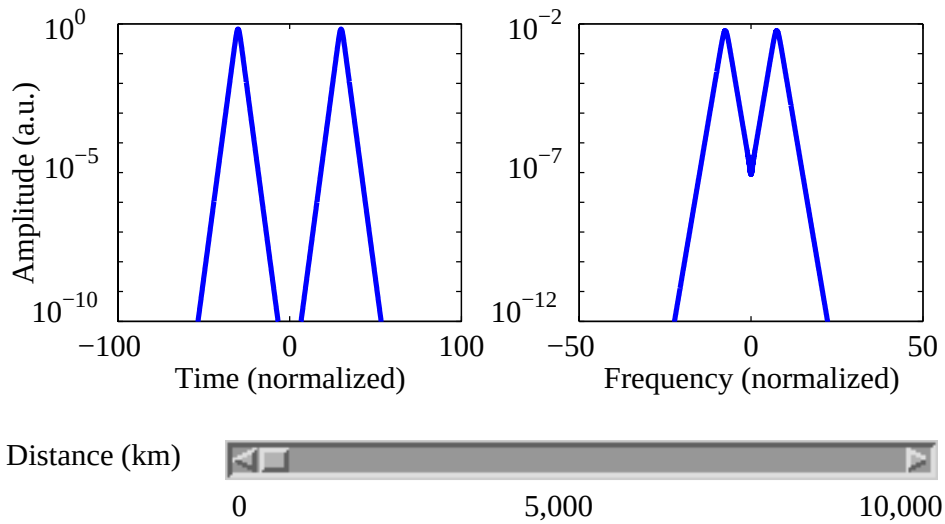

Figure 1. (240 kB) Animation of a two-soliton collision. The normalized frequency spacing is 15, corresponding to 210 GHz.

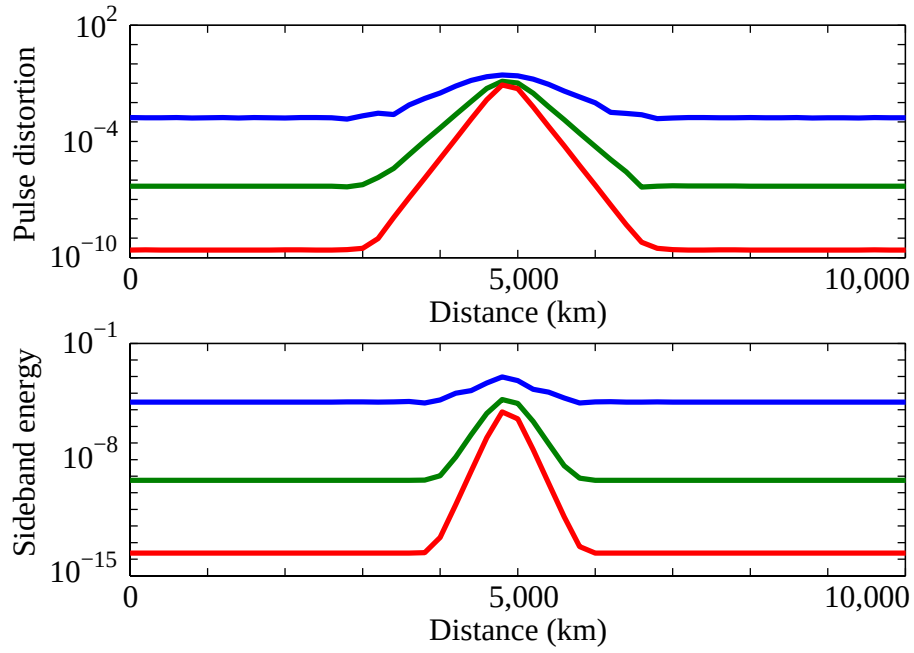

Figure 2. Evolution of the pulse distortion $\delta(z)$ and sideband energy $\varepsilon(z)$ with distance in two-soliton collisions. The blue, green and red curves correspond to frequency separations of 70, 140 and 210 GHz respectively.

#35042 - $15.00 US
Received August 27, 2001; Revised September 18, 2001
(C) 2001 OSA

constant dispersion and nonzero loss compensated with lumped periodic amplification, we would observe resonant growth of four-wave mixing contributions [11]. However, we consider solitons in lossless fibers which are equivalent to a system with dispersion-tapered, lossy fiber [4]. Figure 2 shows the dependence of the four-wave mixing products on propagation distance. Different curves correspond to different frequency separations of the two solitons. The pulse distortion and sideband energy both grow as the pulses start to overlap. They reach their maxima at the point of maximum overlap around 5000 km, and they finally decay to a vanishing background. The initial ($z = 0$) values of the sideband energy computed using (3) are nonzero since, although the power spectrum of the soliton pair is extremely small in the sideband interval $\Omega_{\rm sb}$, it is not identically zero. Moreover, the initial value of the sideband energy $\varepsilon_{\rm sb}(z = 0)$ increases as the frequency separation between the two pulses decreases because the central frequencies of the sidebands become closer to those of the channels. The pulse distortion $\delta(z)$ is also nonzero at the start, since the spectrum of a two-pulse signal around ω_1 is different from the spectrum of a single pulse at ω_1, *i.e.*, in (4), $|\widetilde{q}(z,\omega)| - |\widetilde{q}_1(z,\omega)| \neq 0$ for $\omega \in \Omega_1$, even if the two pulses are far from the collision point.

The behavior of dispersion-managed solitons differs significantly. We show a two pulse collision in the animation in Fig. 3. The sidebands rise as the pulses move towards each other and stay at essentially the same level after the pulses separate. This key difference from the behavior of classical solitons is caused by dispersion management and the presence of loss and amplification, which introduce discontinuity into the system and destroy the symmetry of the collisions. Note that in contrast to the classical soliton case, in which there is a single collision, the use of dispersion management causes the pulses to move back and forth with respect to each other, colliding many times. Figure 4 shows the growth and saturation of the sideband energy in the DMS system. Dispersion-managed solitons tend to recover their shapes after the collision by shedding radiation, but the pulse distortion is only partially compensated. We stress, that when we speak of dispersion-managed solitons, we are referring to periodically stationary pulses in dispersion maps in which sections of large positive and large negative dispersion alternate. In the presence of loss, it is also possible to manage the dispersion by reducing its magnitude exponentially while keeping the dispersion anomalous [4]. In this case, one can mathematically transform the equations that govern the system so that they are identical to the equations that govern classical solitons, and the behavior is like that of classical solitons, rather than like that of the periodically-stationary, dispersion-managed solitons that we are studying here.

By contrast, we find that collisions of two pulses in the DMS system resemble the collision of two pulses in the CRZ system, rather than those in the classical soliton system. We show an animation of a two-pulse collision in the CRZ system in Fig. 5. As in the DMS system, we find that the sidebands do not decay after the collision. The explanation for this behavior in the CRZ system is the same as for the DMS system: Dispersion management, fiber loss, and amplification leave no chance for a collision to be symmetric and for the four-wave mixing products to cancel out. The plots in Fig. 6 show the growth and saturation of $\delta(z)$ and $\varepsilon(z)$, as in the case of the DMS system. The rapid growth of the pulse distortion and sideband energy around 2000 km is consistent with the pulse dynamics of the CRZ format. The pulses spread at the beginning of the propagation after dispersion pre-compensation; they then compress in the middle of the transmission line, spread out again, and finally compress at the end in the dispersion post-compensation fiber [6]. Since the efficiency of four-wave mixing is proportional to the third power of the signal intensity, the sidebands grow significantly when the CRZ pulses are most compressed. By contrast, DMS pulses broaden and compress within one map, periodically reproducing their shape. Thus, a pulse has a larger peak power on

#35042 - $15.00 US Received August 27, 2001; Revised September 18, 2001
(C) 2001 OSA

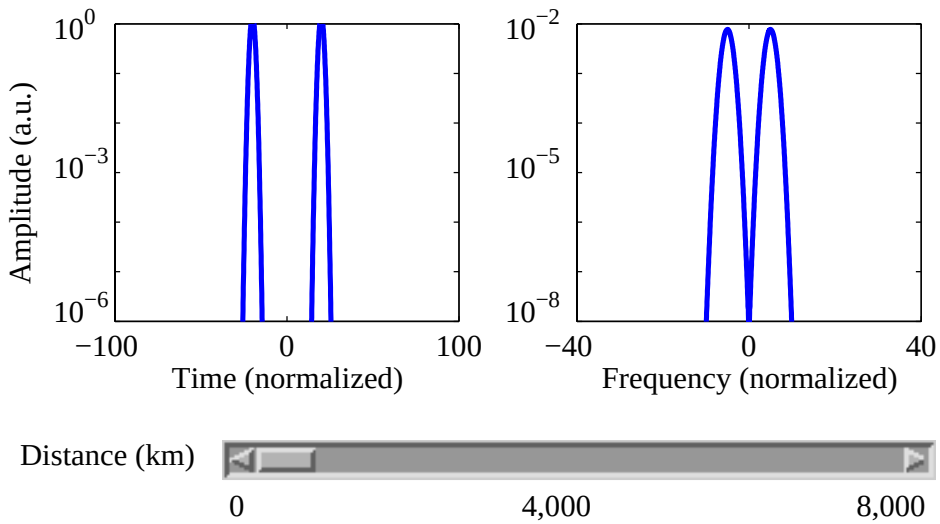

Figure 3. (256 kB) Animation of a two-pulse collision in the DMS system. The normalized frequency spacing is 10, corresponding to 140 GHz.

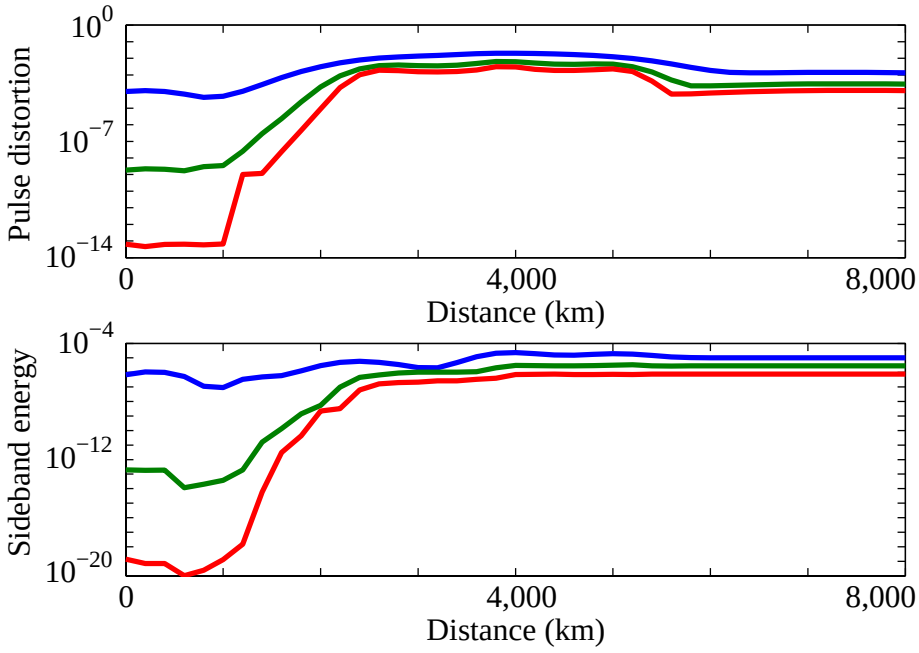

Figure 4. Evolution of the pulse distortion $\delta(z)$ and sideband energy $\varepsilon(z)$ with distance in the DMS system. The blue, green and red curves correspond to the frequency separations of 70, 140 and 210 GHz respectively.

#35042 - $15.00 US
Received August 27, 2001; Revised September 18, 2001
(C) 2001 OSA

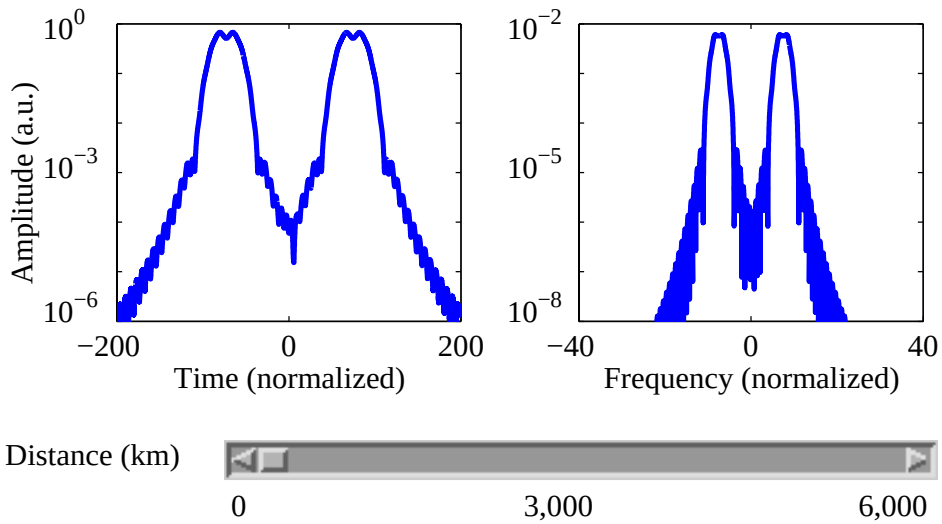

Figure 5. (180 kB) Animation of a two-pulse collision in the CRZ system. The normalized frequency spacing is 15, corresponding to 210 GHz.

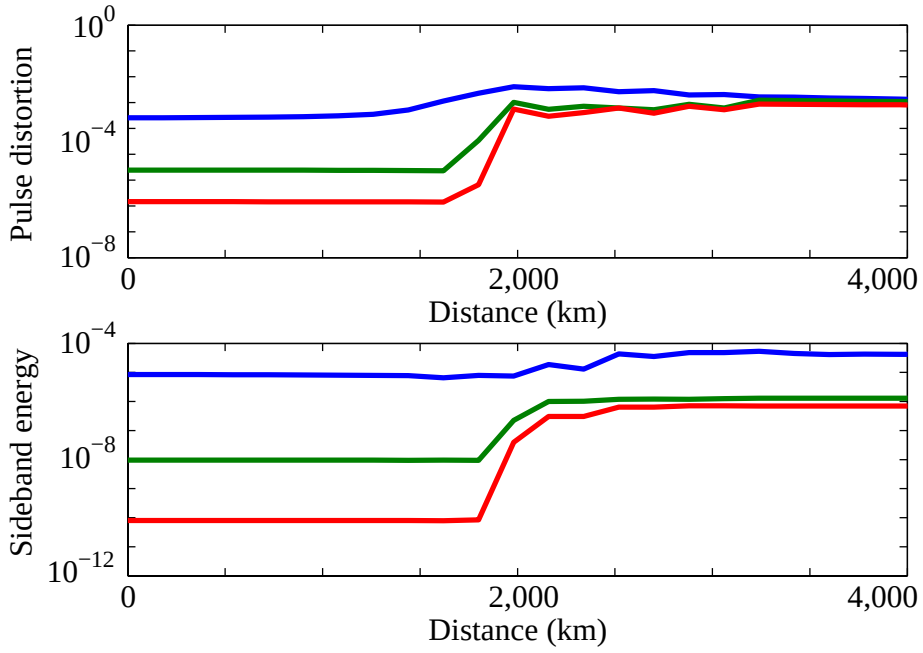

Figure 6. Evolution of the pulse distortion $\delta(z)$ and sideband energy $\varepsilon(z)$ with distance in the CRZ system. The blue, green and red curves correspond to frequency separations of 70, 140 and 210 GHz respectively.

#35042 - $15.00 US
Received August 27, 2001; Revised September 18, 2001
(C) 2001 OSA

average in the DMS system than in the CRZ system, resulting in a higher four-wave mixing efficiency along the whole transmission link. Nonetheless, the basic behavior in which pulse distortion and sideband energy, once created, do not disappear is the same in both the DMS and CRZ systems.

3.2 *Three channel interactions*

Generally, as channels are added to a WDM system, the interchannel interaction becomes stronger and the system performance degrades. A notable exception is the N-soliton solution of the nonlinear Schrödinger equation, for which it has been shown that pulse distortions grow from a vanishing background and then decay back to zero [10]. We show this behavior in an animation in Fig. 7. Moreover, the time shifts that occur in an N-soliton collision are just the sums of the time shifts from the pairwise collisions [12]. The situation is quite different for the DMS and CRZ systems. The animations in Figs. 8 and 9 illustrate that the sidebands do not decay after the collision as in a soliton system. We show the difference between two and three pulse interactions in the DMS and CRZ systems in Figs. 10 and 11 where we plot the sideband energy and pulse distortion for two and three pulses a long distance after the collision point, and we plot these values as a function of frequency spacing. The red curves correspond to the two-pulse case. In case of three pulses the values of the sideband energy and pulse distortion depend on the initial phase of the center pulse. We compute the values of pulse distortion and sideband energy for fifty different initial phases and display the mean plus standard deviation in green and the mean minus standard deviation in blue. This approach allows us to characterize the average behavior of the system. We can clearly see the difference between two- and three-pulse interactions. The effect of a three-pulse collision is worse than that of a two-pulse collision for both the DMS and CRZ systems. This behavior is qualitatively consistent with what we would anticipate from a simple physical picture in which the four-wave mixing interactions increase because the sideband frequencies are now interfering with the signal frequencies [13].

3.3 *Performance of two, three, and five channels with pulse streams*

The difference between two, three, or five WDM channels becomes more critical when we consider a stream of pulses rather than a single pulse in each channel. We used a random 64-bit pattern, which repeats periodically. The optical signal is filtered with a 30 GHz optical Gaussian filter followed by a fifth-order Bessel electrical filter with an 8 GHz FWHM. The channel spacing is 60 GHz in the classical soliton and DMS systems and it is 40 GHz in the CRZ system. The animation in Fig. 12 demonstrates the evolution of the eye diagram with distance for the DMS system. The left, middle, and the right parts of the animation show the electrical eye of the central channel for two, three and five channel systems respectively. The eye closes faster with three channels and even faster with five. Again, this behavior is qualitatively consistent with what we would expect from a simple physical picture in which the four-wave mixing interactions increase because the number of sideband frequencies interfering with the signal frequencies grows rapidly with the number of channels [13]. We note that four-wave mixing is not the only nonlinear effect that causes degradation. Self-phase modulation and cross-phase modulation can also contribute to the signal degradation. However it is not possible to unambiguously distinguish distortions due to four-wave mixing from those due to self- and cross-phase modulation since they are all manifestations of the Kerr effect. We observe nearly identical behavior in the CRZ system (see Fig. 13). By contrast, the animation in Fig. 14 presents the simulation results for multichannel soliton systems with

#35042 - $15.00 US Received August 27, 2001; Revised September 18, 2001
(C) 2001 OSA

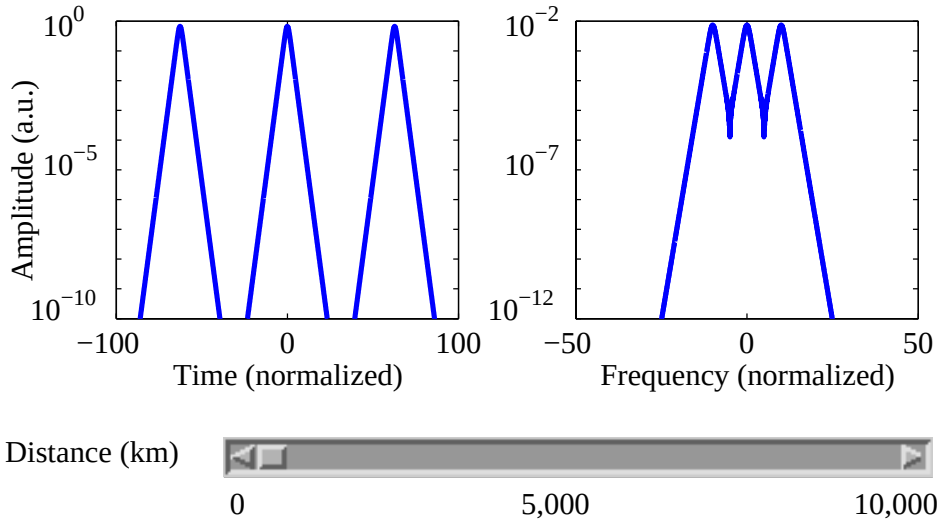

Figure 7. (396 kB) Animation of a three-soliton collision. The normalized frequency spacing is 10, corresponding to 140 GHz.

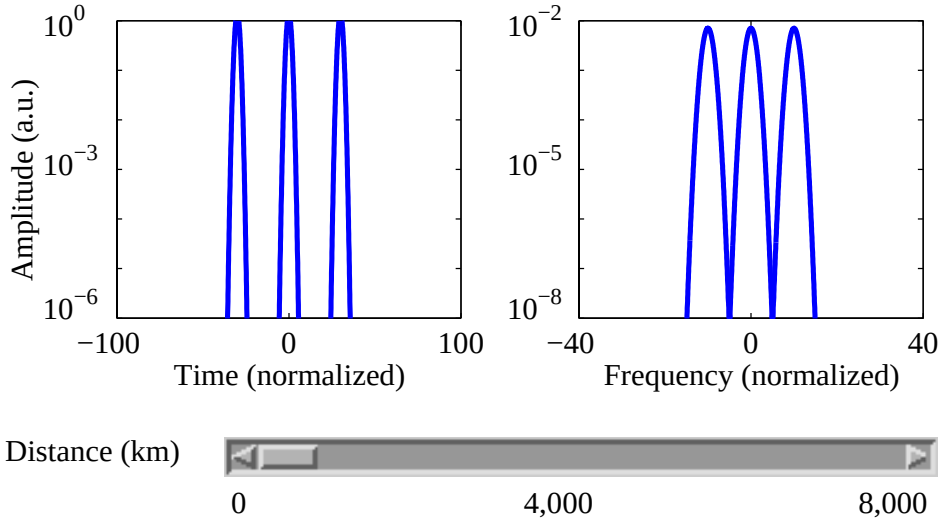

Figure 8. (228 kB) Animation of a three-pulse collision in the DMS system. The normalized frequency spacing is 10, corresponding to 140 GHz.

#35042 - $15.00 US
Received August 27, 2001; Revised September 18, 2001
(C) 2001 OSA

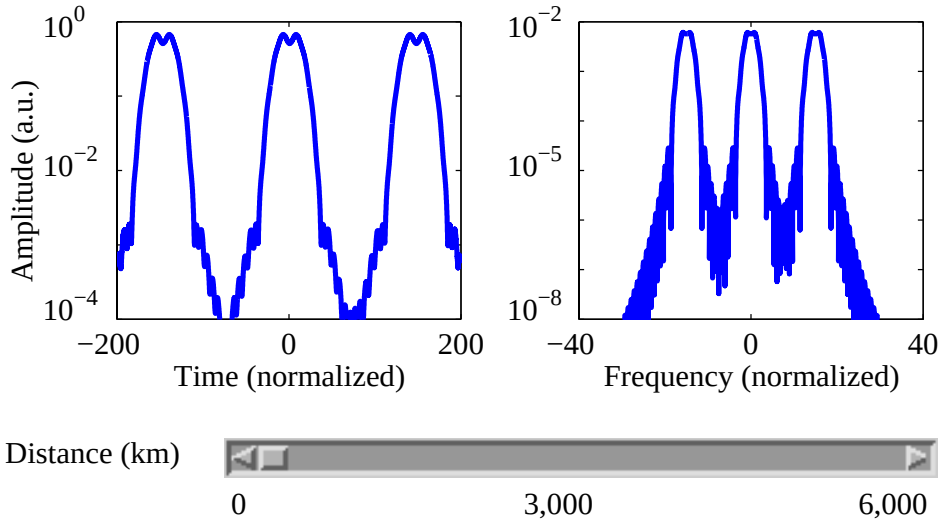

Figure 9. (204 kB) Animation of a three-pulse collision in the CRZ system. The normalized frequency spacing is 15, corresponding to 210 GHz.

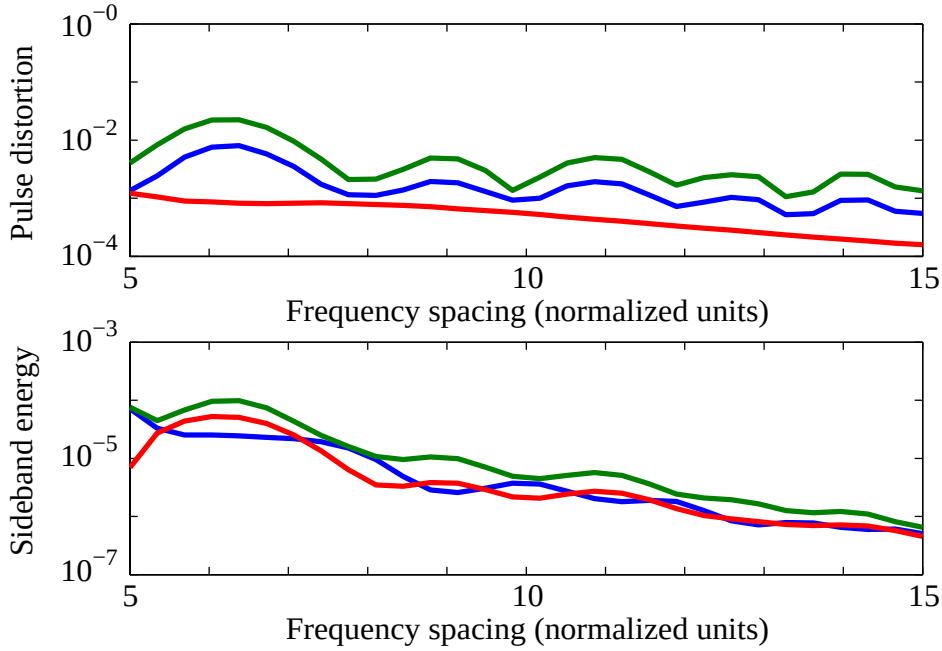

Figure 10. Dependence of the pulse distortion and sideband energy on the channel spacing in the DMS system. The green and blue curves correspond to the mean plus standard deviation and the mean minus standard deviation for the three-pulse interactions. The red curve corresponds to the two-pulse collision.

#35042 - $15.00 US
Received August 27, 2001; Revised September 18, 2001
(C) 2001 OSA

two, three and five channels. We note that there is no visible difference in eye closure among the three cases. There are three major reasons for the eye closure that does occur in the classical soliton system. First, unlike the case with two- and three-pulse collisions, the pulses in different channels are continuously colliding with each other. There are thus incomplete collisions, which degrade the eyes. Second, although the sideband energy is reabsorbed during a soliton collision, the pulses experience a timing shift that also degrade the eyes [12]. Third, intersymbol interference at the demultiplexing filter also contributes to the eye degradation. However, the key point we show here is that there is no visible difference in eye closure as the number of channels increases in the classical soliton system, in contrast to the DMS and CRZ systems.

4 Conclusion

In this work we have compared pulse interactions in classical soliton, DMS, and CRZ systems. Collisions of classical solitons are completely elastic. Although the pulses distort and sideband energy is created during collisions, the pulses are restored to their original shape and the sideband energy is reabsorbed after the collision. By contrast, for pulse collisions in the DMS and CRZ systems, the pulse distortion and sideband energy that are created during collisions remain after the pulses separate. In classical soliton systems, the behavior is fully described as a superposition of pairwise collisions. By contrast, in both DMS and CRZ systems, the behavior grows conspicuously worse as the number of channels increases. We have employed an animation technique to demonstrate that adding new channels in a WDM dispersion-managed system decreases the performance, while it does not in the classical soliton system. We have also shown that the collision dynamics are qualitatively the same in the CRZ and DMS systems. In both those cases, the behavior is consistent with what we would anticipate from a simple physical picture in which the four-wave mixing interactions increase as the number of channels grow.

#35042 - $15.00 US Received August 27, 2001; Revised September 18, 2001
(C) 2001 OSA

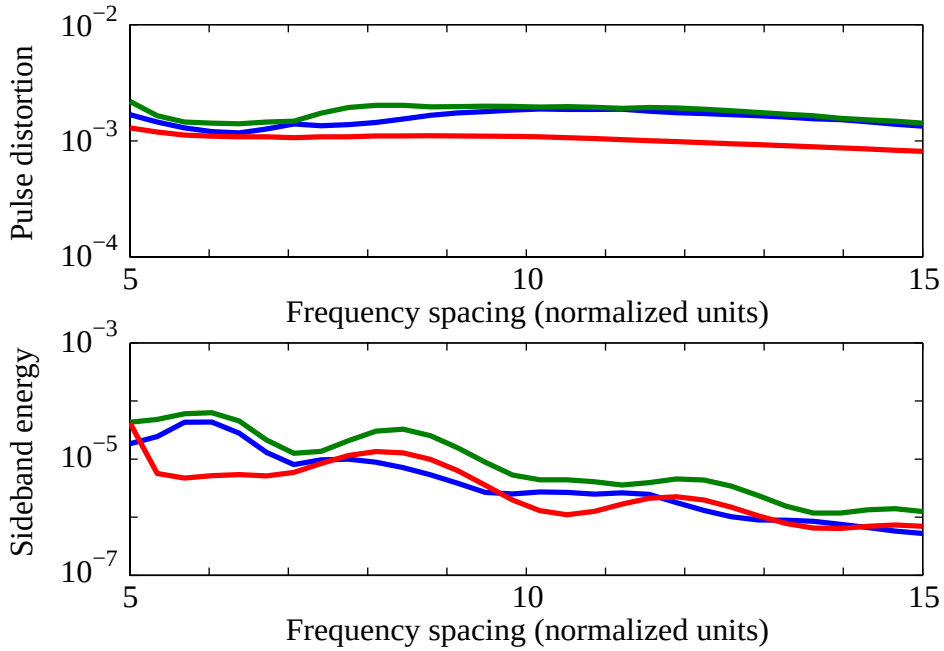

Figure 11. Dependence of the pulse distortion and sideband energy on the channel spacing in the CRZ system. The green and blue curves correspond to the mean plus standard deviation and the mean minus standard deviation for the three-pulse interactions. The red curve corresponds to the two-pulse collision.

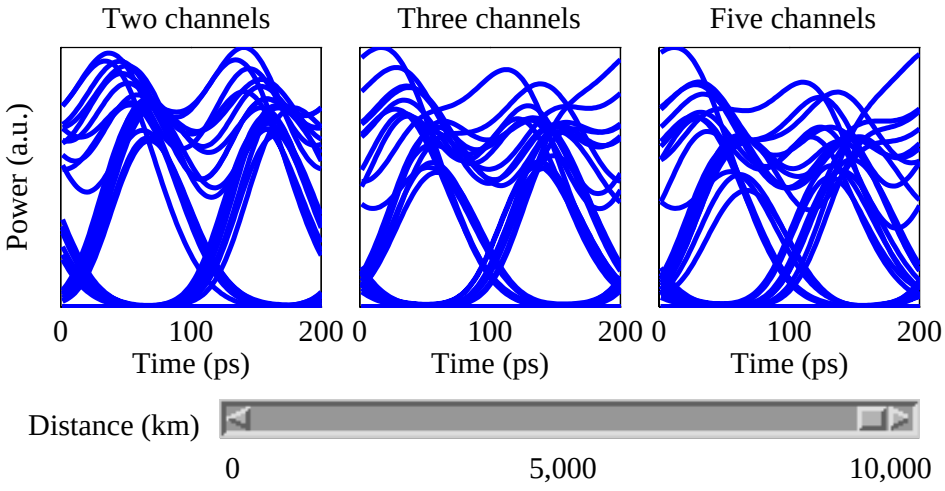

Figure 12. (332 kB animation) Evolution of the electrical eye diagram in the DMS system.

#35042 - $15.00 US
Received August 27, 2001; Revised September 18, 2001
(C) 2001 OSA

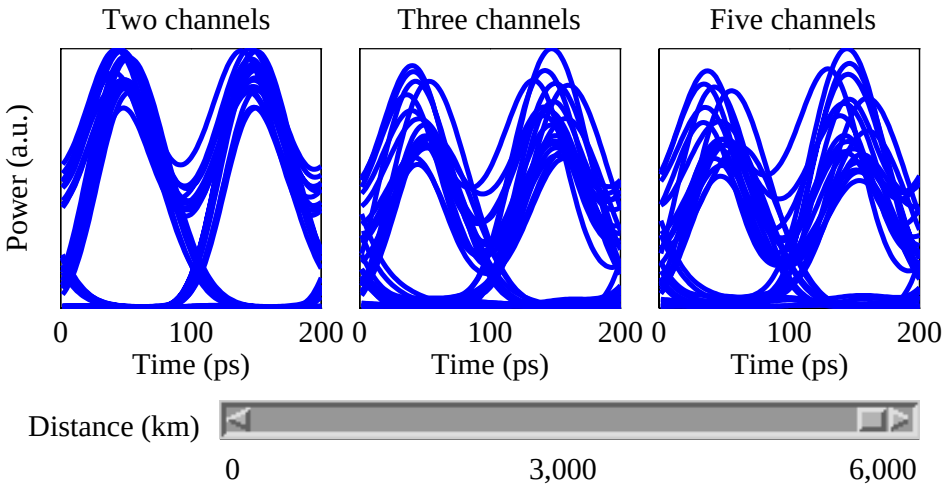

Figure 13. (220 kB animation) Evolution of the electrical eye diagram in the CRZ system.

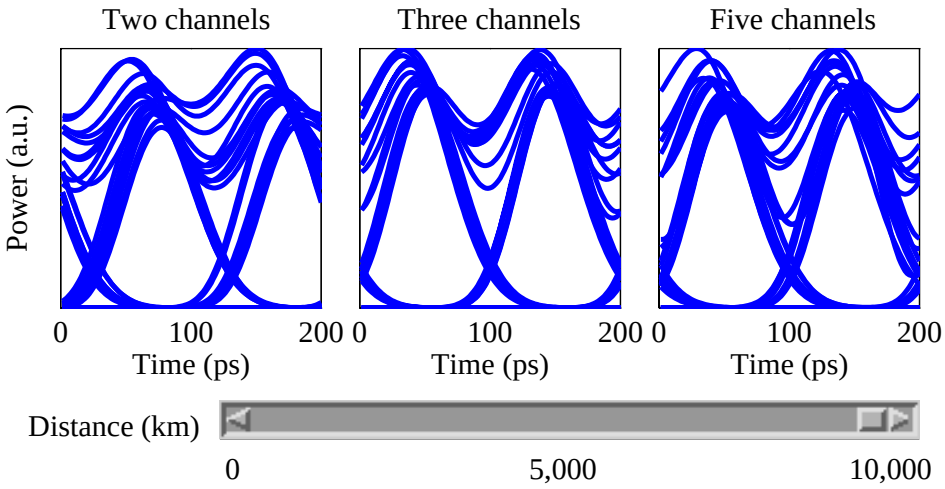

Figure 14. (324 kB animation) Evolution of the electrical eye diagram in the classical soliton system.

#35042 - $15.00 US
Received August 27, 2001; Revised September 18, 2001
(C) 2001 OSA